

RIVETING PROCESS SIMULATION - UPSETTING OF THE MUSHROOM RIVET

Elżbieta Szymczyk, Jerzy Jachimowicz, Grzegorz Sławiński

*Military University of Technology
Faculty of Mechanical Engineering
Department of Mechanics and Applied Computer Science
Kaliskiego 2 Street, 00-908 Warsaw, Poland
tel.: +48 022 683 90 39; fax: +48 022 683 94 61
e-mail: e.szymczyk@wme.wat.edu.pl,
j.jachimowicz@wme.wat.edu.pl
g.slawinski@wme.wat.edu.pl*

Abstract

The paper deals with the analysis of residual stress and strain fields in a riveted joint. This stage of study concerns improving of the fatigue performance of riveted joints in an airframe. Riveting, particularly in aviation, is a traditional but still commonly used method of joining sheet metal components. Aircraft structures are thin-walled ones, with coverings made of thin sheets stiffened by stringers, frames or ribs. Sheets are typically assembled by multiple rivet or bolt joints. Rivets and bolts are also used to joint sheets and stiffeners. Therefore, fatigue resistance of the aircraft structure depends on tens of thousands or even hundreds of thousands rivet joints, which are used to build it. The local numerical models of the joint are considered with regard to the aim introduced in the paper. Numerical FE simulations of upsetting process are carried out using the MARC code. Three-dimensional numerical models are used to determine the resulting stress and strain fields at the mushroom rivet and around the hole. This type of problem requires the use of contact between the elements assembled and non-linear geometric and elasto-plastic multilinear material models to simulate the behaviour of the rivet and sheets. The influence of the squeezing force on strain and stress states is studied. A certain solution to the problem connected with non-uniform stress distribution in the rivet hole is proposed and analysed.

Keywords: Riveted joint, mushroom rivet, FEM local model, stress and strain fields

1. Introduction

Riveting is the oldest and the most popular method of joining metal parts of aircraft structure. It is used in large airliners and freight aircraft (in which number of rivets is counted in millions and their weight may achieve a few tons) and in light fighter-trainers and cargo planes as well as in helicopters in which riveting is the basic method of joining metal components.

Transport planes from 40's and 50's of 19th century like DC-3 or nowadays assembled in Mielec M-28 can be taken as an example. In the newest structure of the European passenger plane Airbus 380 riveting is also the basic method of joining metal parts of fuselage. Conventional and weldable aluminium alloy as well as composite materials e.g. GLARE (glass-reinforced fibre metal laminate) [1, 2] are used to build this structure.

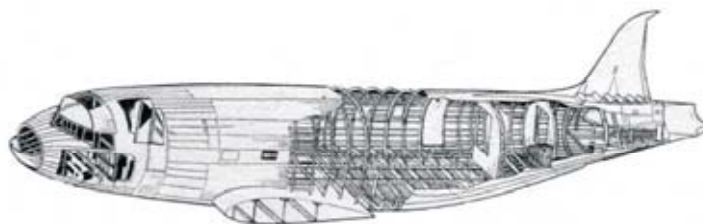


Fig. 1. Monocoque aircraft structure

Thin walled structures named in aircraft monocoque or semimonocoque consist of a frame (stringers and cross stiffeners - ribs or spars) (Fig. 1) that supports other components of the construction. The frame is covered with thin sheets of thickness varying from 0.6 mm to 4 mm. Sheets of covering are joined with stiffeners by rivets or bolts. Recently, welded or adhesive joint is often used.

The residual stress (locally exceeding yield stress level) and plastic strain states are generated in the joint after the riveting process. Residual stress can be defined as the stress state that remains in a part of a structure after all applied forces have been removed. Thermal and mechanical processes like heat treatment, hot or cold rolling, riveting etc. have an influence on the level of residual stresses. The total stress experienced by the material at a given location within a component depends on the residual and applied stress. Residual stress fields are widely accepted to have a significant influence on fatigue life of aircraft structures. Compressive residual stress can be beneficial because it tends to decrease probability of stress corrosion and fatigue cracking [1].

Furthermore, surface coating of contacting bodies has a significant influence on fatigue life of riveted joints. Contact surface is subjected to mechanical, thermal and chemical interaction. External surface of structural elements can be obtained as an effect of cladding and anodising process.

Joining process is performed using riveting press or pneumatic riveter according to aircraft technology. Axisymmetric stress field appears around the rivet hole for properly driven rivet (Fig. 2a). Nonaxial rivet position or other manufacturing imperfections may cause asymmetric stress field (related to the non-uniform distribution of pressure during the riveting process) observed in Fig. 2b [3, 4].

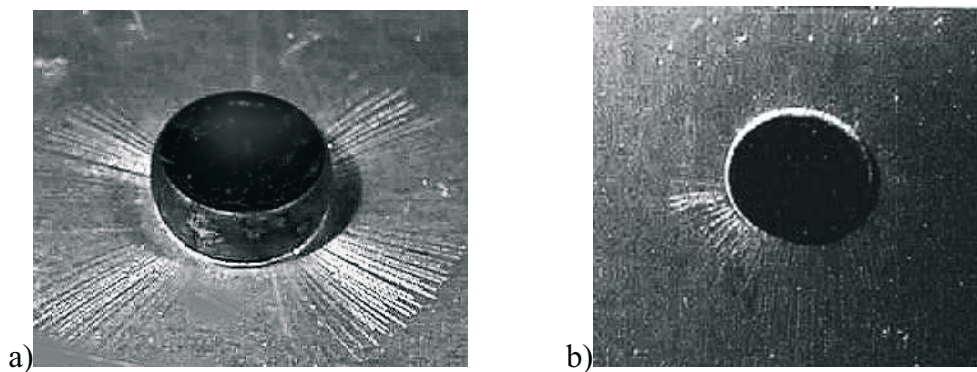


Fig. 2. Visual detection of cracks field around the rivet hole a) properly driven rivet b) effect of non-uniform pressure distribution

2. Numerical model

The analysis is carried out for the solid mushroom rivet (shank diameter $r = 3.5$ mm) joining two aluminium sheets (thickness 1.2 mm). The three-dimensional numerical model of the neighbourhood (10.5 mm wide) of a single rivet is considered (Fig. 3). Dimensions of the mushroom rivet are taken according to Russian standard [OST 1 34040-79] (head radius $R = 4.2$ mm, diameter $D = 7$ mm, height $h = 1.88$ mm). The radius R_p of the rounded tool surface is equal to 4.8 mm.

The models of rivet and sheets consist of eight-noded, isoparametric, three-dimensional brick elements (type Hex8) with tri-linear interpolation [5]. Materials used in riveted joints are subjected to high-strain deformation (plastic deformation). Mechanical tensile and compressive testing is required to determine mechanical property data like: Young's modulus of elasticity, yield strength and nonlinear behaviour of stress - strain curve above the yield stress level. Sheet material (D16TN) is tested for standard flat specimen (in PN-91/H-04310 specification). Tensile and compressive tests are performed for the „rivet” sample.

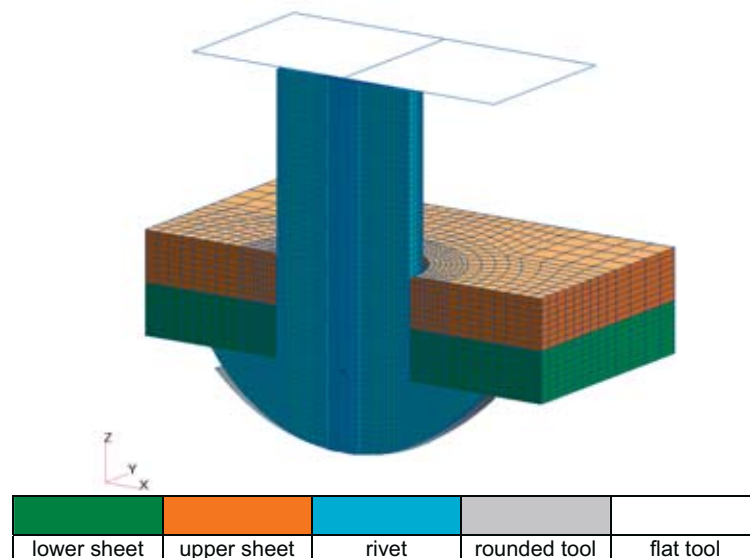


Fig. 3. Model of riveted specimen

Consequently elasto-plastic material models are considered. Multilinear material true stress - logarithmic strain curves [5] for sheet and rivet alloy are presented in Fig. 4. The magnitude of the yield stress and tensile strength are obtained from uniaxial test. The measurement of yielding for the multiaxial state is performed using the von Mises yield criterion.

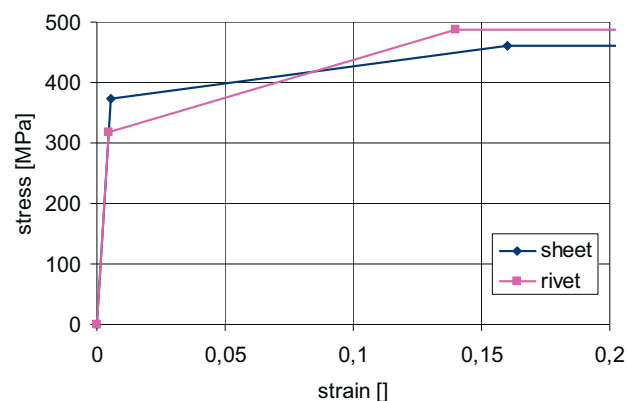


Fig. 4. Nonlinear stress-strain curves

The classical updated Lagrange procedure for elastic-plastic materials and large strain plasticity option is used due to large geometrical and material non-linearities.

The rounded and the flat rivet tools are described as rigid surfaces. The contact with friction is defined between the mating parts of the joint (12 contacted areas). The Coulomb friction model with friction coefficient $\mu = 0.2$ is used.

The penalty method is applied to numerically implement the contact constraints. Iterative penetration checking approach allows to change the contact condition within the Newton-Raphson iteration loop. Using this procedure, the iteration process is done simultaneously to satisfy both the contact constraints and global equilibrium using the Newton-Raphson method. This procedure is accurate and stable, but may require additional iterations.

The outside edge of the sheets are constrained in normal direction. This model describes a part of the multi-riveted joint. The lower (rounded) tool is fixed and the upper one is moved a given distance down.

Two load steps are considered: step I - upsetting the rivet, step II - unloading (removing the riveter).

3. Numerical calculations

The numerical calculations are performed for four cases of upsetting (w1, w2, w3, w4) described by the height of the formed rivet head (Tab. 1).

Tab. 1. Formed rivet head dimensions

| | w1 | | w2 | | w3 | | w4 | |
|---------------------------|------|-----|------|-----|------|-----|------|-----|
| | [mm] | [%] | [mm] | [%] | [mm] | [%] | [mm] | [%] |
| head height $h, h/h_0$ | 2.1 | 50 | 1.9 | 45 | 1.65 | 39 | 1.5 | 36 |
| head diameter $D, D/d$ | 4.9 | 140 | 5.18 | 148 | 5.5 | 157 | 5.75 | 164 |

The formed rivet diameter and the rivet hole filling capability depend on the rivet head height [6]. The nominal rivet head diameter ($D = 1.5d$) and the tolerance limits ($\pm 0.1d$) are specified in manufacturing instruction of riveting. The following formed rivet head diameters are approached (as a result of numerical simulations): for case w1 - the minimum allowable value, for case w2 - the average (nominal) value, for case w3 - the maximum allowable value. The minimum tolerant rivet head height is obtained for case w4, but its diameter exceeds the allowable value. Rivet deformations and plastic strain fields are given in Fig. 5.

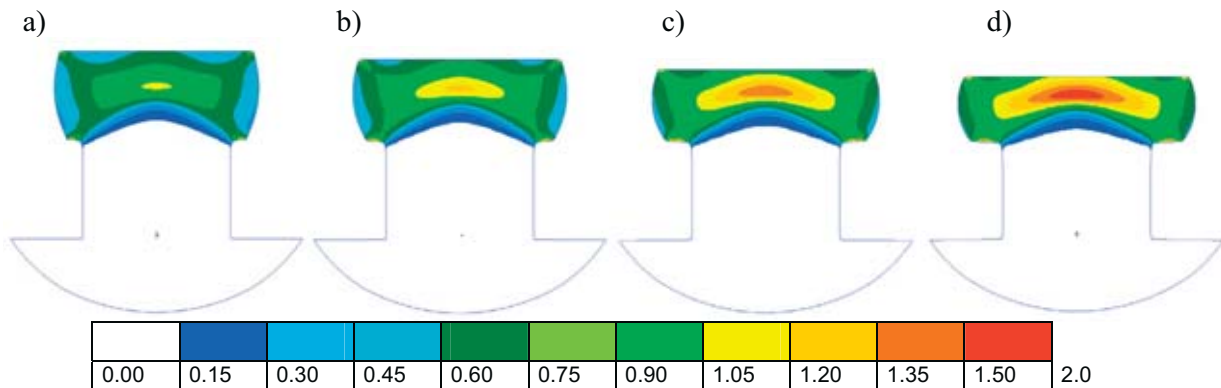


Fig. 5. Rivet deformations and plastic strain fields a) w1 b) w2 c) w3 d) w4

Irreversible plastic deformations of sheet material around the rivet hole remain after the riveting process as a result of the rivet shank swelling in the hole. The fields of the radial and the hoop stress components in the middle surface of the upper (Fig. 6-8) and the lower sheet (Fig. 7-9) after I (pressure) and II (unloading) load steps are presented in the figures. The absolute values of stresses in the upper sheet (from the side of the formed rivet head) are about 20% greater than corresponding values in the lower sheet. The relative differences in stress values between sheets rise to 25% after unloading (load step II). Extreme negative values of the radial stresses occur at the rivet hole and tend to decrease with increase of the radial distance from the hole [7]. The hoop stress values are positive in the elastic range. During upsetting process and growth of plastic deformations band around the rivet hole the hoop stress values became locally substantially negative (Fig. 8-9).

The curves of radial, hoop and axial stresses as well as plastic strains versus radial distance from the rivet hole are shown in Fig. 10 and 11. The presented stress and strain values in the middle surfaces of the sheets are obtained for case w4.

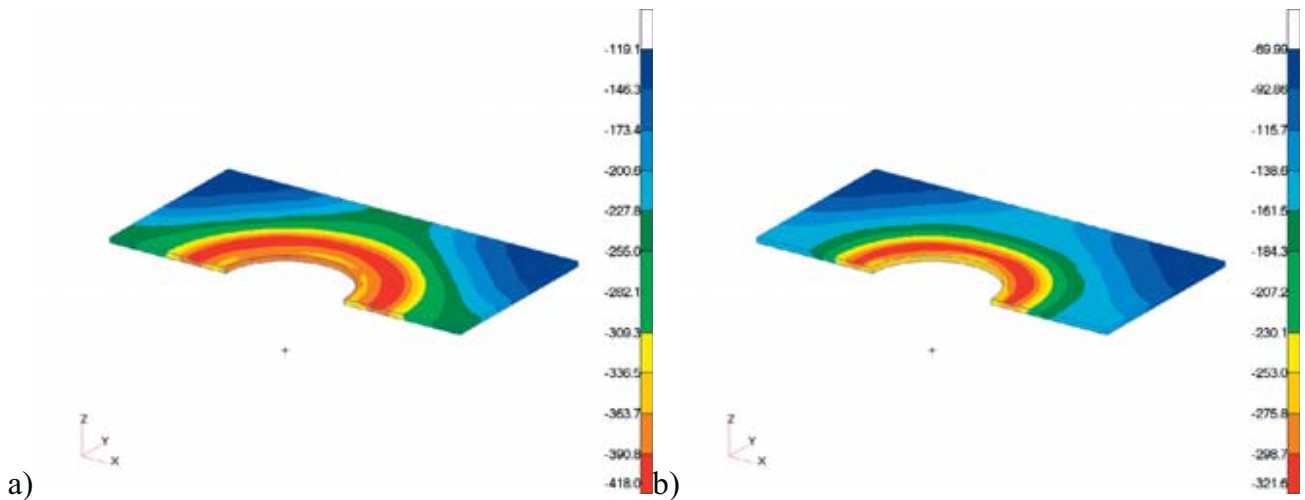


Fig. 6. Radial stresses in the upper sheet a) pressure b) unloading

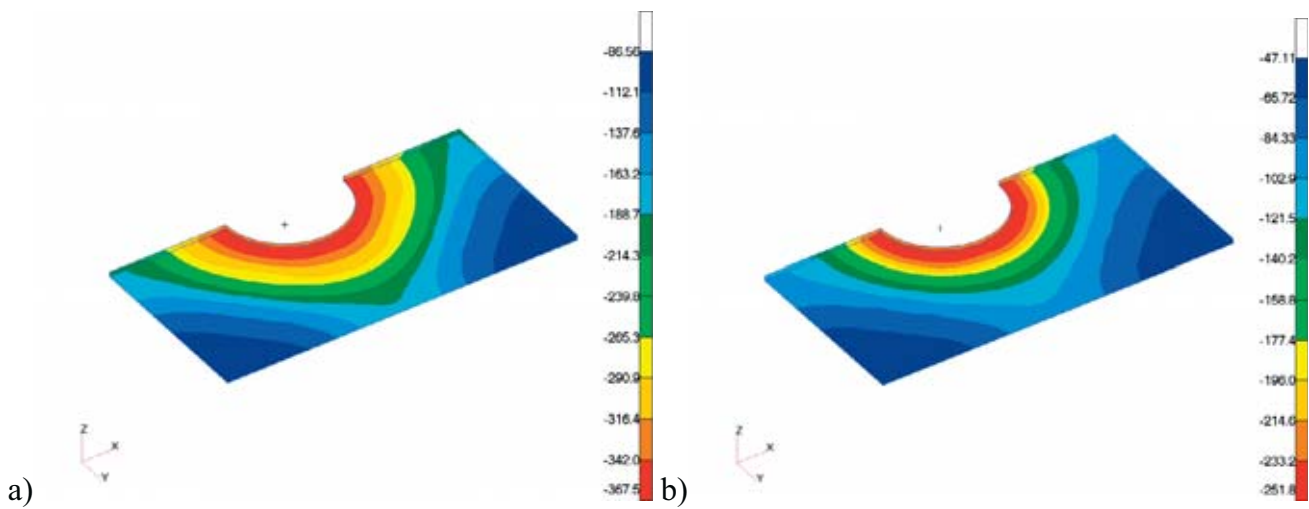


Fig. 7. Radial stresses in the lower sheet a) pressure b) unloading

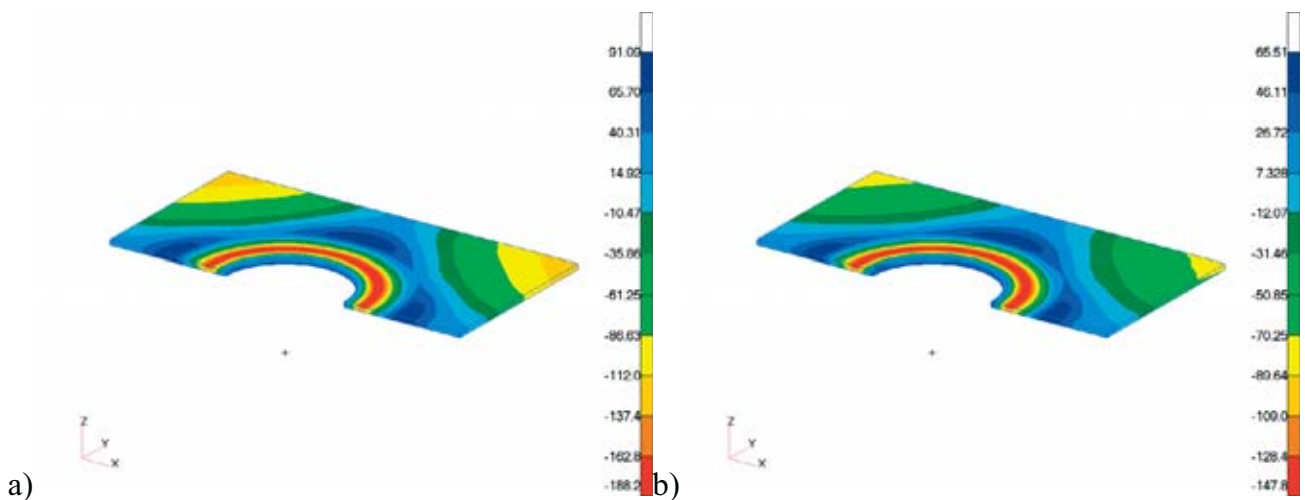


Fig. 8. Hoop stresses in the upper sheet a) pressure b) unloading

The radial stress values after load step I (pressure) are about 100 MPa greater than the residual stresses. Those values in the upper sheet are about 50 MPa greater than corresponding values in the lower one. The hoop and axial stress fields are not so regular. Curves for the upper and the lower sheets have different nature. The maximum compressive stress in hoop direction for the lower sheet occurs at the rivet hole, whereas that for the upper sheet appears about 0.5 mm from the hole (under the formed rivet head).

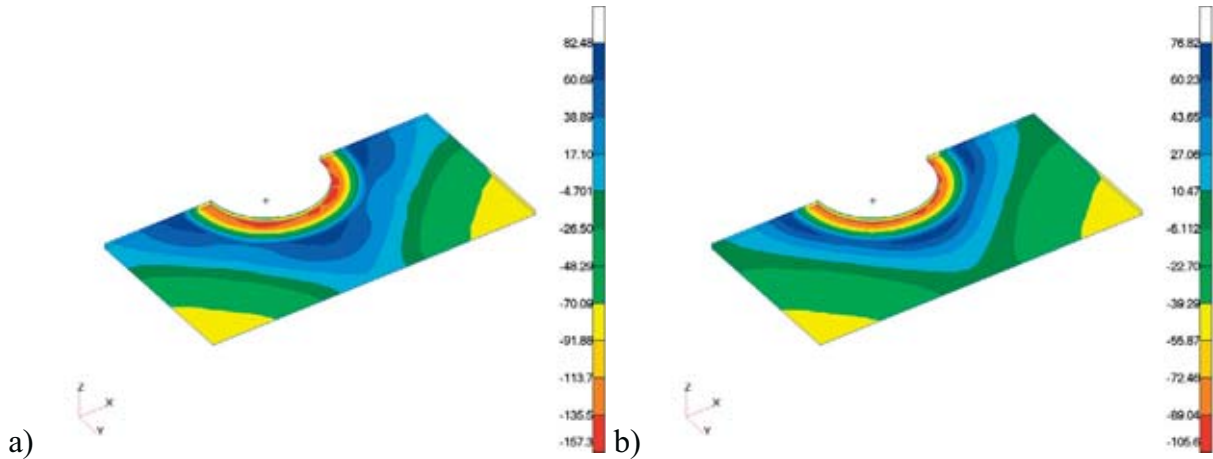


Fig. 9. Hoop stresses in the lower sheet a) pressure b) unloading

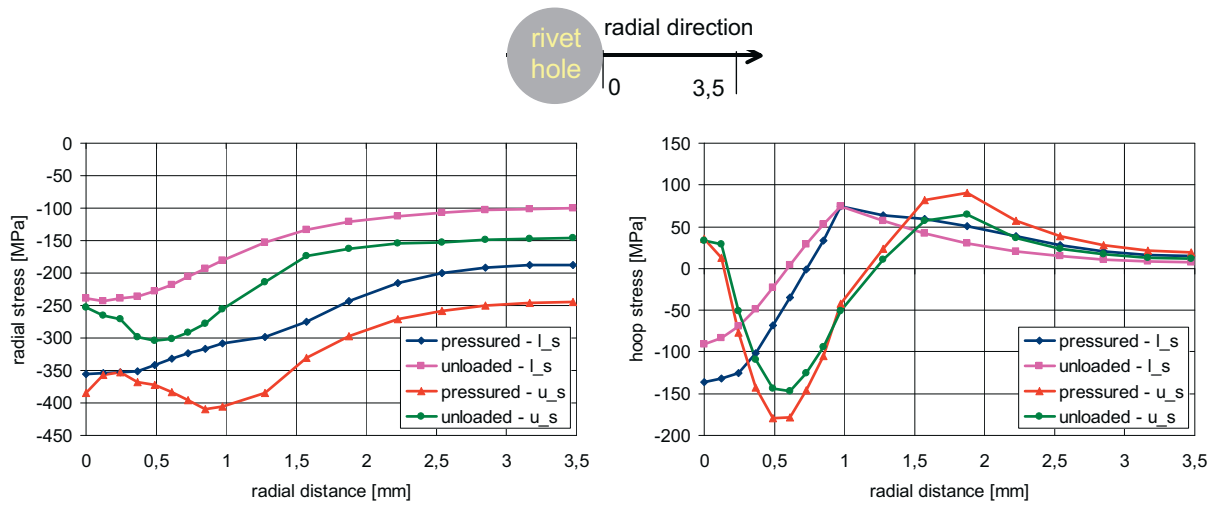


Fig. 10. Stress values vs. radial distance from the hole a) radial stress b) hoop stress

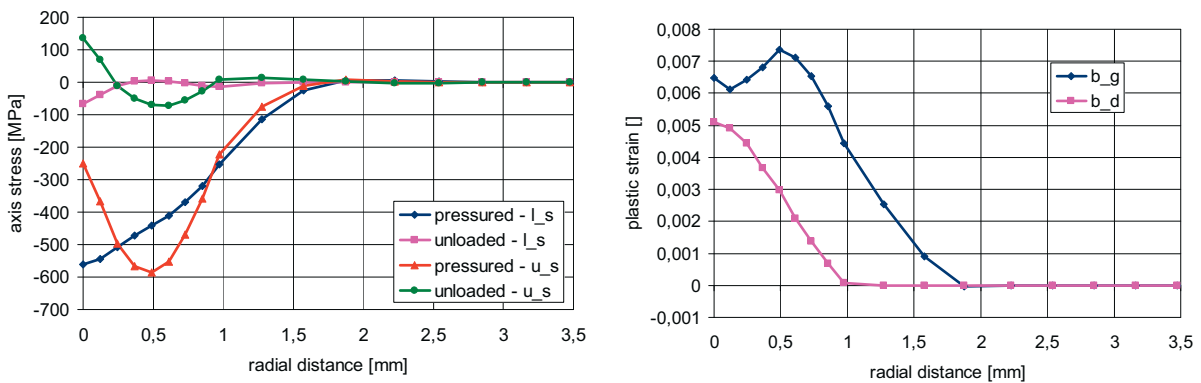


Fig. 11. Result values vs. radial distance from the hole a) axial stress b) plastic strain

In other cases of upsetting (case w1-w3) the resultant curves are similar. The comparison of results for various head height are presented in Fig. 12-17.

The decrease in the formed rivet head height results in a regular increase in the absolute values of the radial stresses (Fig. 12-13). Significant changes of the hoop and axial stresses occur under the rivet head only (Fig. 14-17). The hoop stresses fields in the lower sheet seem to be more beneficial than in the upper one, because the extreme negative values occur at the rivet hole (Fig. 14b). Regrettably, the compression (on the level of - 100 MPa) takes place only for case w4, when the head diameter exceeds the allowable value. For the upper sheet, extreme negative values

of the hoop stresses appear about 0.5 mm from the rivet hole (Fig. 15b), but they are on the level of - 50 MPa (for case w2) and - 120 MPa (for case w3).

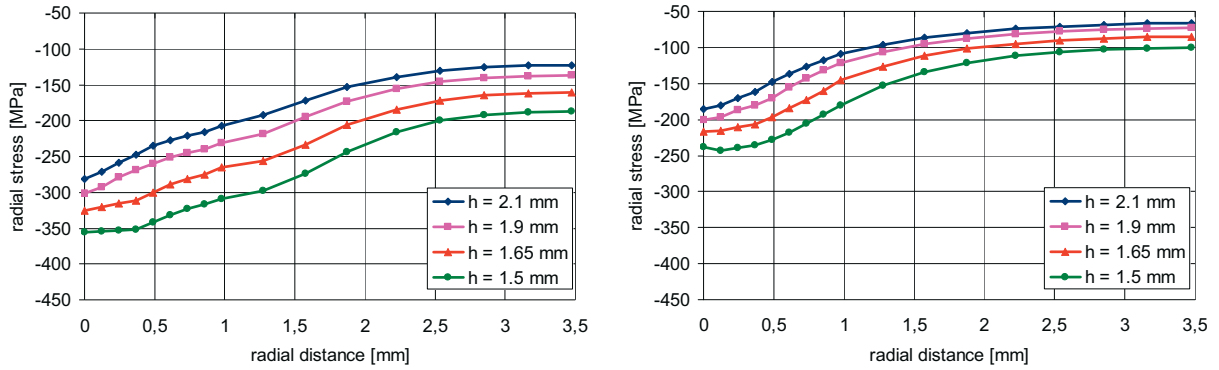


Fig. 12. Radial stress values vs. radial distance from the hole (lower sheet) a) pressure b) unloading

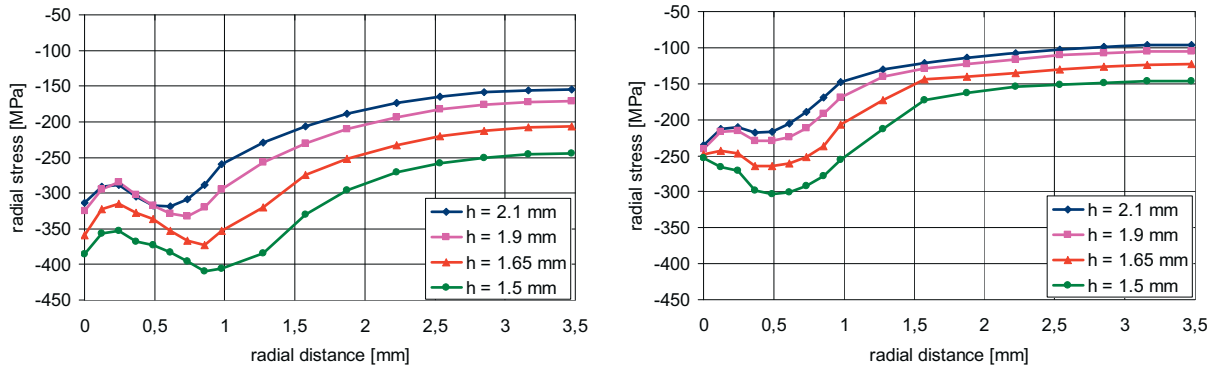


Fig. 13. Radial stress values vs. radial distance from the hole (upper sheet) a) pressure b) unloading

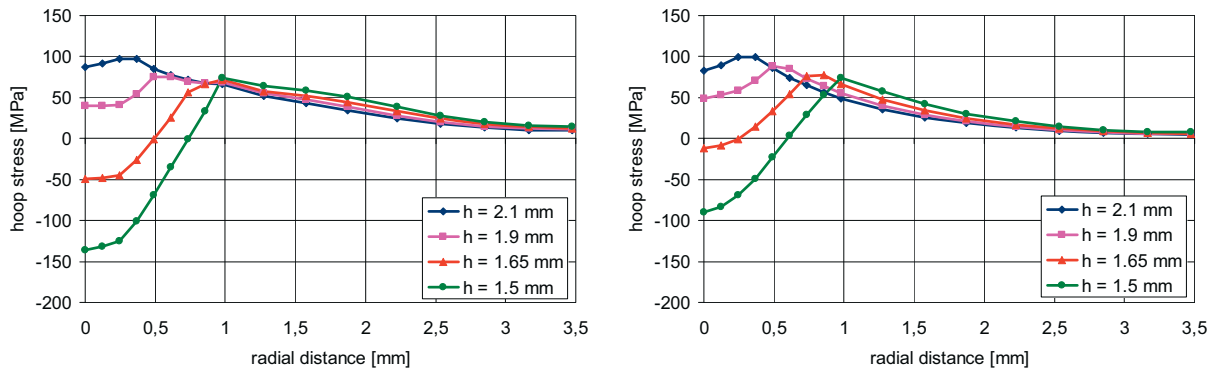


Fig. 14. Hoop stress values vs. radial distance from the hole (lower sheet) a) pressure b) unloading

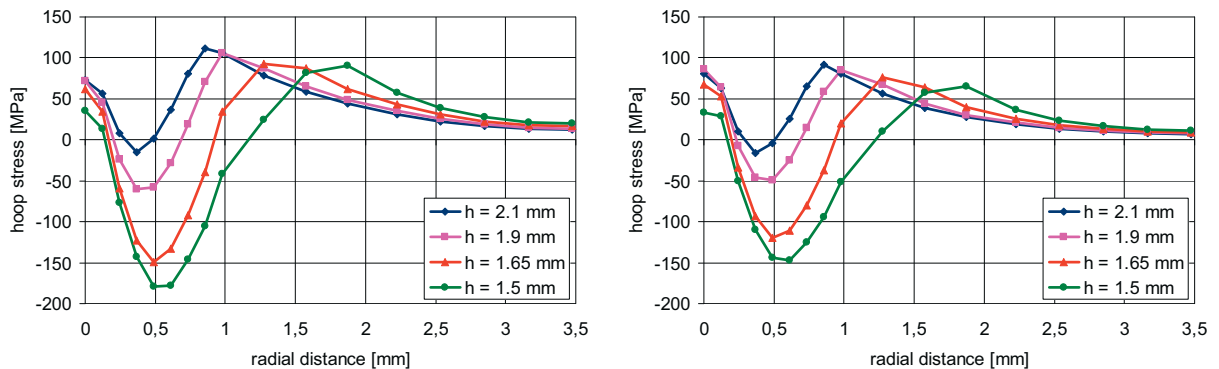


Fig. 15. Hoop stress values vs. radial distance from the hole (upper sheet) a) pressure b) unloading

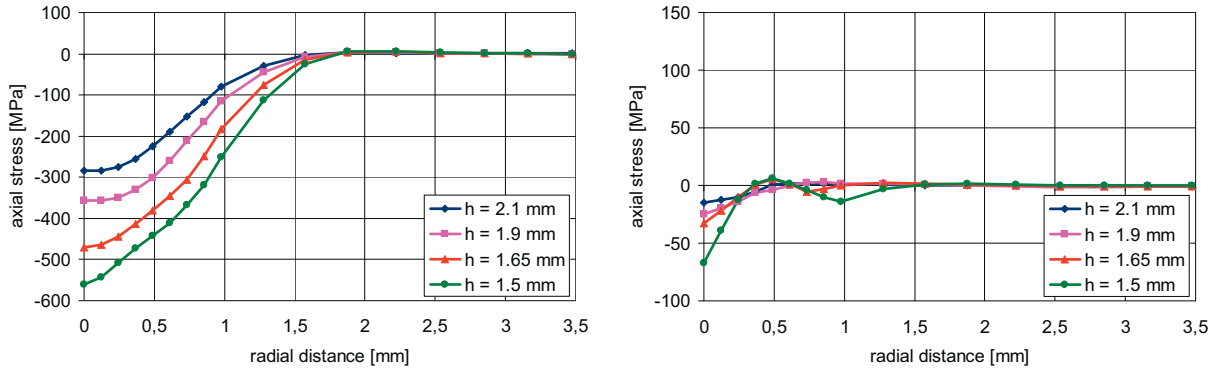


Fig. 16. Axial stress values vs. radial distance from the hole (lower sheet) a) pressure b) unloading

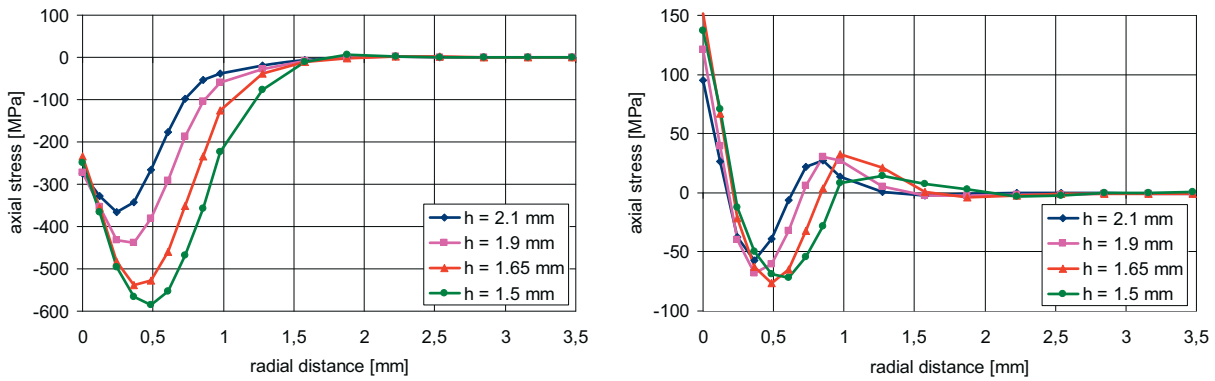


Fig. 17. Axial stress values vs. radial distance from the hole (upper sheet) a) pressure b) unloading

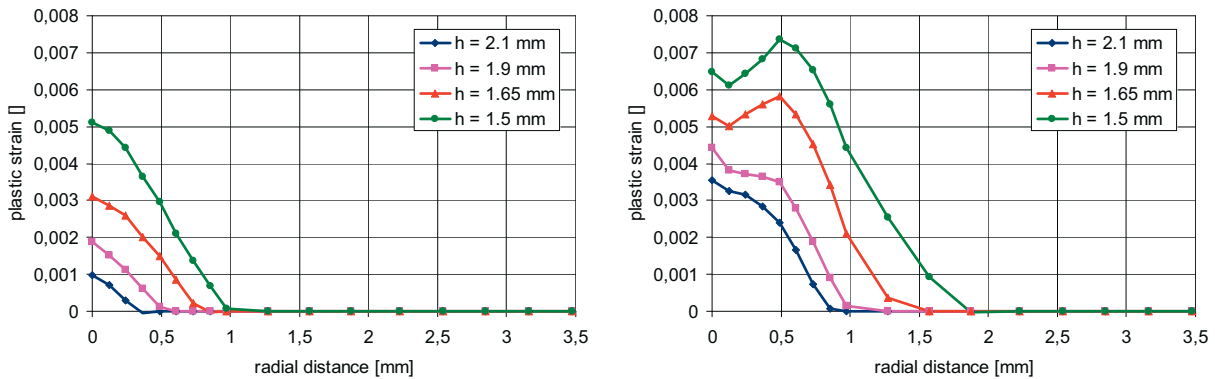


Fig. 18. Plastic equivalent strain values vs. radial distance from the hole a) lower sheet b) upper sheet

The plastic deformation region in the middle surface of the lower sheet is two times smaller than the corresponding region of the upper sheet (Fig. 18).

3.1. Modified model

Some modification of the riveting process based on squeezing the rivet with restriction of the formed head dimension is proposed in paper [8]. In case w5, the upsetting rivet head height attain 1.65 mm (as in case w3), while the rivet head diameter is restricted (limited) to 5.18 mm (as in case w2). This modification causes a better rivet hole filling capability. The radial and hoop stress curves versus radial distance from the hole are presented in Fig. 19. Plastic strain curves for upper and lower sheets are shown in Fig. 20.

Unlike previous results, for case w5 the stress values in upper and lower sheets are at the same level (Fig. 19). Stress values after unloading are about 40% greater than corresponding values for case w4. Maximum plastic strain is at the same level as for case w2, whereas almost the whole analysed rivet neighbourhood in both sheets is in plastic state (Fig. 20).

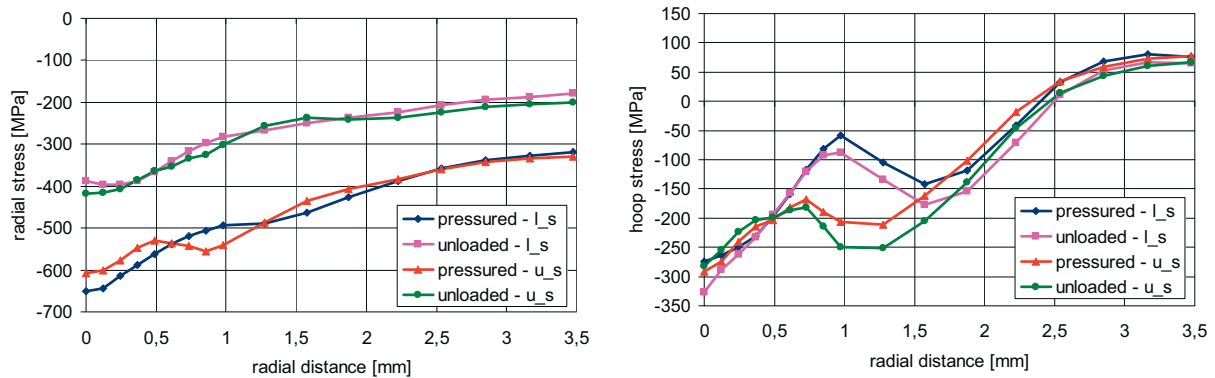


Fig. 19. Stress values vs. radial distance from the hole (case w5) a) radial stress b) hoop stress

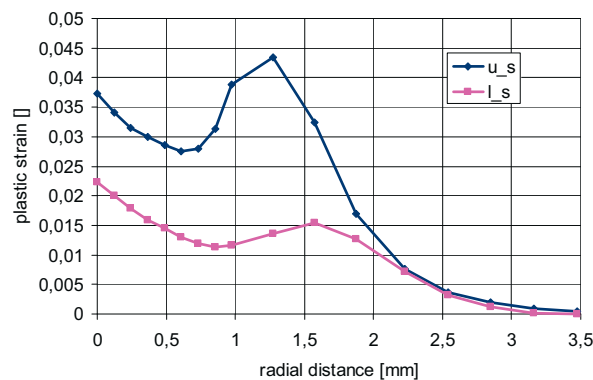


Fig. 20. Plastic strain values vs. radial distance from the hole – case w5

4. Conclusions

Numerical FE simulations of the upsetting process are carried out using the MARC code. Stress and strain fields in the neighbourhood of the rivet hole are analysed for various squeezing conditions.

The formed rivet diameter and the rivet hole filling capability depend on the rivet head height. Irreversible plastic deformations of sheet material around the rivet hole remain after the riveting process as a result of the rivet shank swelling in the hole. The absolute values of stresses in the upper sheet (from the side of the formed rivet head) are about 20% greater than corresponding values in the lower sheet. The relative differences in stress values between sheets rise to 25% after unloading (load step II).

The decrease in the formed rivet head height (increase in the squeezing force) results in a regular increase in the absolute values of the radial stresses. Significant changes of the hoop and axial stresses occur under the rivet head only. The plastic deformation region in the middle surface of the lower sheet is two times smaller than the corresponding region of the upper sheet.

With regard to the manufacturing process, a certain solution to the problem connected with nonuniform stress distribution in the rivet hole is analysed. This modification causes a better rivet hole filling capability. The stress values in upper and lower sheets are at the same level. The plastic deformation covers almost the whole analysed rivet neighbourhood in both sheets.

Acknowledgements

This work was carried out with the financial support of Polish Ministry of Science and Higher Education under research project in the framework of the Eureka Initiative.

References

- [1] Muller, R., *An experimental and numerical investigation on the fatigue behaviour of fuselage riveted lap joints*, Doctoral Dissertation, Delft University of Technology, 1995
- [2] de Rijck, J., *Stress Analysis of Fatigue Cracks in Mechanically Fastened Joints*, Doctoral Dissertation, Delft University of Technology, 2005
- [3] Szymczyk, E., Jachimowicz, J., Derewońko, A., *Analysis of residual stress fields in riveted joint*, Journal of KONES, Vol. 14, pp. 465-474, Warszawa 2007
- [4] Jachimowicz, J., Kajka, R., Szachnowski, W., Szymczyk, E., *FEM and experimental analysis of strain and stress states around the rivet hole in the thin walled aircraft structure* (in polish), *Analizy numeryczne wybranych zagadnień mechaniki*, 21, 399-424, Warszawa 2007.
- [5] MSC Marc Theoretical Manual, MSC Corp. 2007.
- [6] de Rijck J, Homan J.J., Schijve J., Benedictus R., *The driven rivet head dimensions as an indication of the fatigue performance of aircraft lap joints*, International Journal of Fatigue 29 (2007) 2208-2218.
- [7] Szymczyk, E., Derewońko, A., Kiczko, A., J. Jachimowicz, *Numerical simulation of tensile loaded lap riveted joint*, Journal of KONES, Warszawa 2006
- [8] Szymczyk, E., Jachimowicz, J., Sławiński, G., Derewońko, A., *Numerical modelling and analysis of riveting process in aircraft structure*, (in polish), IX Międzynarodowa Konferencja Naukowa COMPUTER AIDED ENGINEERING, Szklarska Poręba 2008